molecular pharmaceutics

Article

pubs.acs.org/molecularpharmaceutics

Phase Separation Behavior of Fusidic Acid and Rifampicin in PLGA Microspheres

Samuel E. Gilchrist,[†] Deborah L. Rickard,[‡] Kevin Letchford,[†] David Needham,[‡] and Helen M. Burt*[,†]

[†]Faculty of Pharmaceutical Science, University of British Columbia, Vancouver, British Columbia V6T 1Z3, Canada

[‡]Department of Mechanical Engineering and Materials Science, Duke University, Durham, North Carolina 27708, United States

Supporting Information

ABSTRACT: The purpose of this study was to characterize the phase separation behavior of fusidic acid (FA) and rifampicin (RIF) in poly(D,L-lactic acid-*co*-glycolic acid) (PLGA) using a model microsphere formulation. To accomplish this, microspheres containing 20% FA with 0%, 5%, 10%, 20%, and 30% RIF and 20% RIF with 30%, 20% 10%, 5%, and 0% FA were prepared by solvent evaporation. Drug−polymer and drug−drug compatibility and miscibility were characterized using laser confocal microscopy, Raman spectroscopy, XRPD, DSC, and real-time video recordings of single-microsphere formation. The encapsulation of FA and RIF alone, or in combination, results in a liquid−liquid phase separation of solvent-and-drug-rich microdomains that are excluded from the polymer bulk during microsphere hardening, resulting in amorphous spherical drug-rich domains within the polymer bulk and on the microsphere surface. FA and RIF phase separate from PLGA at relative droplet volumes of 0.311 ± 0.014 and 0.194 ± 0.000, respectively, predictive of the incompatibility of each drug and PLGA. When coloaded, FA and RIF phase separate in a single event at the relative droplet volume 0.251 ± 0.002, intermediate between each of the monoloaded formulations and dependent on the relative contribution of FA or RIF. The release of FA and RIF from phase-separated microspheres was characterized exclusively by a burst release and was dependent on the phase exclusion of surface drug-rich domains. Phase separation results in coalescence of drug-rich microdroplets and polymer phase exclusion, and it is dependent on the compatibility between FA and RIF and PLGA. FA and RIF are mutually miscible in all proportions as an amorphous glass, and they phase separate from the polymer as such. These drug-rich domains were excluded to the surface of the microspheres, and subsequent release of both drugs from the microspheres was rapid and reflected this surface location.

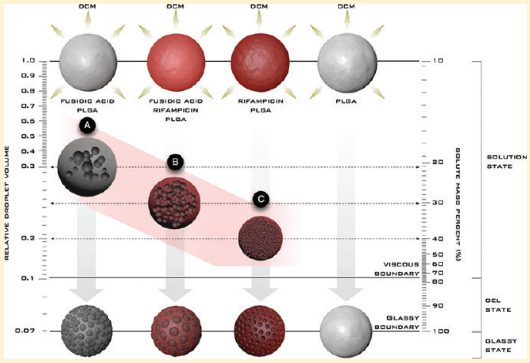

KEYWORDS: *fusidic acid, rifampicin, controlled-delivery, microspheres, phase separation, PLGA*

INTRODUCTION

Polymeric microspheres composed of the polyesters poly(lactic acid) and poly(lactic acid-*co*-glycolic acid) (PLGA) copolymers, loaded with a wide range of drugs, have been the subject of extensive studies over the past three or four decades.[1] Drug loaded microspheres injected subcutaneously, intramuscularly, or locally at target sites can provide controlled release of bioactive agents over days, weeks, or months to treat a variety of disease states.[2−6] Accordingly, there are several successful marketed PLGA microsphere formulations loaded with drugs, such as leuprolide acetate, triptorelin pamoate, octreotide acetate, lanreotide, risperidone, naltrexone, and exenatide, for the treatment of a range of conditions, including alcohol dependence, prostate cancer, acromegaly, endometriosis, and type II diabetes.[7]

Recently, our group examined the loading of fusidic acid (FA), an antimicrobial agent active against a number of Gram positive microorganisms, including *S. aureus*, *S. epidermidis*, and coagulase negative *staphylococci*, including strains that are methicillin resistant, into PLGA microspheres for potential application for the controlled and localized delivery of FA to sites of orthopedic infection.[8] In these studies, a very distinctive microsphere morphology was observed as a result of phase separation of FA from PLGA as FA-rich, amorphous microdomains producing uniform and spherical protrusions on the microsphere surface. During microsphere formation, PLGA and FA were codissolved in the organic solvent dichloromethane (DCM). Upon formation of the initial oil in water emulsion, DCM rapidly leaves the dispersed phase, diffusing into the surrounding aqueous, continuous phase. Consequently, the polymer and FA solution concentrates, and just before solidification of the polymer, a FA-rich DCM phase appears to separate. Using a variety of techniques, including real-time recording of single-microsphere formation, it was shown that coalescence of these liquid FA-rich microdroplets, throughout the forming microsphere and at the interface, resulted in the appearance and growth of rounded protrusions at the surface.[8]

Received: February 16, 2012
Revised: March 30, 2012
Accepted: April 7, 2012
Published: April 7, 2012

This same phenomenon has also been observed by two other groups studying the encapsulation of cyclosporine A in PLGA microspheres[9,10] and was described as "islands" of drug surrounded by the polymer matrix. It was suggested by both groups that the "islands" were composed of amorphous phase-separated drug, based on the fact that the "island" diameters increased with increasing drug loading. We agree with this conclusion, and our single microsphere studies directly demonstrated a similar phase separation process for FA.[8]

Phase separation of drug within the polymer matrix and at the surface of microspheres can occur during fabrication, most commonly using the solvent evaporation method, and has been extensively reported.[11,12] It is well established that drug may precipitate in the polymer in a crystalline form or as an amorphous form within the carrier.[13−16] Interestingly, phase separation may be accompanied by changes in microsphere morphology from the completely smooth surfaces observed for control (no drug) microspheres to a concave dimpled appearance, as in, for example, paclitaxel loaded poly(L-lactic acid) microspheres[14] and progesterone loaded PLGA microspheres,[15] or "rough" or "porous" surfaces, as in, for example, quinidine loaded poly(D,L-lactic acid) microspheres[13] and peptide loaded PLGA microspheres.[17] Phase separation of drug in a number of binary and ternary solvent-cast films has also been reported.[18−21]

Several reports have shown surface-associated drug phase separation from the polymer matrix, after the microspheres have been formed. However, there are only a few reports attempting to explain the underlying mechanisms of formation behind these phenomena. DeLuca and co-workers have carried out detailed kinetic and thermodynamic modeling of the formation of polymeric microspheres using the solvent evaporation method, and the processes underlying the formation of porous microspheres.[22,23] In these investigations, porous microspheres were formed when salmon calcitonin peptide was loaded into PLGA microspheres using dichloromethane (DCM) as solvent and methanol as a cosolvent (to dissolve the loaded peptide). The authors explain that as solvent is transported out of the liquid phase droplet, the liquid droplet becomes increasingly viscous and eventually forms a gel at what is termed the viscous boundary (VB). Loss of more solvent results in crossing the glassy boundary, eventually leading to a glassy state composed of solid polymer and drug.[22] Using a ternary phase diagram of DCM, methanol, and PLGA, Li et al.[23] described the droplet phase composition changing with solvent loss and two phases being produced as the viscous boundary is approached, referred to as a polymer-rich phase, containing primarily polymer and solvent with small amounts of cosolvent and drug, and a polymer-poor phase, containing the bulk of the drug. Pores within the resulting microspheres were postulated to be due to the peptide, either trapping absorbed cosolvent (methanol), and/or imbibed continuous phase (water) in the bulk matrix or dissolved peptide in water adsorbing onto PLGA via hydrophobic bonding.[23] Using the micropipet techniques discussed in this investigation, it is possible to view, in real time, the events of phase separation to confirm or refute any of these postulated mechanisms.

An understanding of the phase behavior of drugs and methods to study these phenomena in polymeric carriers is critical for the optimization of drug-delivery formulations, as phase separation can impact drug release profiles and drug stability. We have expanded our investigations of the phase separation phenomena of FA from PLGA microspheres to include dual FA and rifampicin (RIF) loaded microspheres. RIF is active against *S. aureus* and *S. epidermidis*, but it also shows activity against *Streptococcal* organisms (including *Streptococcus pneumoniae*), *Clostridium welchii*, *Neisseria meningitidis*, and *Pasteurella multocida*.[24,25] The broad spectrum of activity of both FA and RIF confers protection against ≥70% of organisms that commonly cause prosthetic joint infections,[26] and thus there is considerable clinical use of combinations of FA and RIF in implant associated orthopedic infections.[27,28] Therefore, a combination product that provides controlled release of FA and RIF at the site of infection may be of clinical benefit. In this work, we explore the ternary phase separation behavior and the miscibility characteristics of FA and RIF in PLGA microspheres prepared by solvent evaporation from DCM, and we bring a new mechanistic understanding to these complex, and thus far unseen, phase separation behaviors using real-time video recording of forming microspheres.

MATERIALS

Fusidic acid (FA), rifampicin (RIF), and poly(vinyl alcohol) (PVA; 98% hydrolyzed; MW 13−23 g/mol) were purchased from Sigma Aldrich (Oakville, ON, CA). Poly(D,L-lactic acid-*co*-glycolic acid) (PLGA; 50:50) with a number-averaged molecular weight (M_n) of 49,100 Da was purchased from Lactel Absorbable Polymers (Pelham, AL, USA). The solvents dichloromethane (DCM), acetonitrile (ACN), methanol (MeOH), and phosphoric acid, were of HPLC grade and purchased from Sigma Aldrich (Oakville, ON, CA). Micropipets were made from borosilicate glass capillaries (0.75 mm (o.d.), 0.4 mm (i.d.) × 6 in. (A-M Systems, Inc., Everett, WA, USA)).

METHODS

Fabrication of Antibiotic-Loaded PLGA Microspheres. Drug loaded PLGA microspheres were prepared by an oil-in-water (O/W) single emulsion and solvent evaporation method. Briefly, PLGA (50:50), FA, and/or RIF were codissolved at various concentrations in 5 mL of DCM to achieve a final combined drug−polymer concentration of 10% (*w*/*v*). Ratios were 20% FA with 0%, 5%, 10%, 20%, and 30% RIF and 20% RIF with 30%, 20% 10%, 5%, and 0% FA. The drug/PLGA solution was then added dropwise into a flask containing 100 mL of 2.5% (*w*/*v*) aqueous PVA solution with overhead propeller stirring at 600 rpm (BDC 2002; Caframo, Wiarton, ON, CA) to form the O/W emulsion. The resulting emulsion was stirred continuously for 2.5 h at room temperature to evaporate the organic solvent. The microspheres were allowed to sediment in the flask on the benchtop for 5 min and subsequently washed three times with distilled water with benchtop sedimentation for 5 min to remove unencapsulated drug, residual DCM, and PVA. The microspheres were then dried under 635 mmHg vacuum at room temperature for 24 h using a benchtop vacuum oven (Napco No. 5831) and stored in a desiccator until further analysis.

Microsphere Particle Size Distribution. The mean particle size and size distributions of FA, RIF, and FA-RIF-co-loaded PLGA microspheres were determined using a Malvern Mastersizer 2000 laser diffraction particle size analyzer (Malvern Inc., Malvern, Worcestershire, U.K.). Briefly, approximately 5 mg of microspheres was weighed and suspended in 5 mL of distilled water along with two drops of 1% polysorbate 80 (Tween 80) and sonicated for 2 min to

prevent aggregation of microspheres. The particle size distribution of microspheres was expressed as mean diameter along with the span, where the span is calculated according to the following equation:

$$\text{span} = \{[\text{diameter at 90\% cumulative size}] - [\text{diameter at 10\% cumulative size}]\} / [\text{diameter at 50\% cumulative size}] \quad (1)$$

Drug Encapsulation Efficiency. To determine the encapsulation efficiency of the FA and RIF antibiotics, ~2.5 mg of antibiotic-loaded microspheres was weighed and dissolved in 1 mL of ACN in a screw-top test tube with a Teflon-coated cap. Five milliliters of phosphate buffered saline (PBS; pH 7.4) was added, and the resulting solution was mixed via vortex for 60 s to precipitate the polymer. The solution was centrifuged at 18,000*g* (Microfuge 18; Beckman Coulter, Mississauga, ON, CA) for 5 min to pellet any precipitate, and the supernatant was sampled for FA and RIF content.

The FA content of the dissolved PLGA microspheres was quantified using a HPLC (Waters Millennium System) assay utilizing a mobile phase of 50/30/20 (*v*/*v*/*v*) ACN/MeOH/0.01 M phosphoric acid solution, flowing at 1 mL/min through a C18 reverse phase Nova-Pak column (Waters), with a 20 μL sample injection volume and UV vis detection at 235 nm. FA was quantified against a standard curve prepared by dissolving FA in ACN over the range 0.1 to 500 μg/mL.

RIF content was evaluated using a UV-spectrophotometer (Varian Cary 50-BIO) assay with a medium scan speed and detection at 475 nm. RIF was quantified against a standard curve prepared by dissolving RIF in DMSO/PBS over the range 0.2–25 μg/mL.

***In Vitro* Drug Release from PLGA Microspheres.** Antibiotic-loaded microspheres were accurately weighed (~5 mg) and placed into 15 mL of PBS (pH 7.4; 0.1 mg/mL ascorbic acid) in screw-top test tubes with a Teflon-coated cap. Ascorbic acid was added to the PBS release media as an antioxidant, since it has been shown to stabilize RIF and prevent oxidative degradation.[29] Each tube was tumbled end-over-end at 10 rpm in a thermostatically controlled oven at 37 °C. At predetermined time intervals, release tubes were removed and centrifuged at 1400*g* (GS-6 Centrifuge; Beckman Coulter, Mississauga, ON, CA) to sediment the microspheres, and 1 mL of the supernatant was withdrawn for HPLC or UV analysis as described above. The remaining media was removed and replaced with fresh PBS (pH 7.4; 0.1 mg/mL ascorbic acid) to maintain sink conditions. The solubility of FA is 5.2×10^{-3} g/L, and that of RIF is 4.13×10^{-2} g/L, and at no point did the concentration of either drug reach these limits during this measurement of drug release from the PLGA microspheres.

Laser Confocal Microscopy. The detailed surface morphologies of the FA, RIF, and coloaded PLGA microsphere formulations were characterized using confocal laser scanning microscopy. Samples were placed on double-sided tape adhered to a glass microscope slide, and images were captured using a LEXT OLS3100 confocal laser scanning microscope (Olympus; Markham, ON, CA).

Raman Spectroscopy. High spatial resolution Raman spectroscopy surface mapping analyses of FA, RIF, and FA-RIF coloaded PLGA microsphere formulations were kindly performed by Dr. Tim Smith of Renishaw, plc (Wotton-under-Edge, U.K.). Specifically, Raman spectra were obtained on a Renishaw RM100 confocal Raman Microscope (Renishaw, plc), recorded at a spatial resolution of 1 μm. Images were subsequently created using a component method (using FA, RIF, and PLGA reference spectra), and images were generated from StreamLine images of an Anadin Extra tablet as a reference with argon ion laser excitation at λ = 785 nm.

X-ray Powder Diffraction. X-ray powder diffraction (XRPD) patterns of FA, RIF, and FA-RIF coloaded microspheres, and physical drug-polymer mixtures were obtained at 25 °C with a Bruker APEX DUO diffractometer equipped with an area detector, cross-coupled multilayer optics, and Cu Kα radiation. Samples were packed into thin-walled capillary tubes (special glass; Charles Supper Company, Natick, MA, USA) and sealed using a small amount of capillary wax. For each sample, three frames of data were collected at different 2θ angles, and the frames were merged together, producing a scan range of 4–60° 2θ. The sample to detector distance was 150 mm, and each sample was rotated 360° about the phi axis with a 5 min data collection time per frame. The data were merged and integrated using Bruker XRD^2 EVAL software and analyzed using the Bruker EVA program.

Differential Scanning Calorimetry. DSC analysis of FA, RIF, and FA-RIF coloaded PLGA microspheres, and physical drug–polymer mixtures was carried out using a TA Instruments DSC Q100 (New Castle, DE, USA) with a liquid nitrogen cooling system. The heat flow and heat capacity of the instrument were calibrated routinely using a high purity indium standard. Briefly, accurately weighed samples between 4–6 mg were hermetically sealed in aluminum pans with a pinhole and heated from 25 to 300 °C at a rate of 10 °C/min under nitrogen flow. The initial heat scan was followed by a rapid quench cooling scan from 300 to −50 °C at a rate of 35 °C/min and a second heating scan from −50 to 250 °C at a rate of 10 °C/min. All DSC thermograms were analyzed using TA Instruments Universal Analysis (v. 4.7A).

DSC was used to determine the ability of FA and RIF to form a miscible blend. FA and RIF were cosolidified from DCM at room temperature in the absence of PLGA. Approximately 5 mg of cosolidified drug was hermetically sealed in aluminum pans with a pinhole and heated from 25 to 300 °C at a rate of 10 °C/min under nitrogen flow. Using published T_g values for FA (117 °C),[8] and RIF (160 °C),[30] the Fox equation, which defines the weight fraction-dependent shift in glass transition temperature of any blend ($T_{g,BLEND}$), was used to generate a reciprocal plot over a range of FA:RIF weight fractions and was plotted along with the experimental T_g values observed in the drug-loaded microspheres and as cosolidified drug. The Fox equation is expressed as follows:

$$\frac{1}{T_{g,BLEND}} = \frac{w_{FA}}{T_{g,FA}} + \frac{w_{RIF}}{T_{g,RIF}} \quad (2)$$

where w_{FA} and w_{RIF} are the weight fractions of FA and RIF and $T_{g,FA}$ and $T_{g,RIF}$ are the glass transition temperatures for FA and RIF, respectively.

Micromanipulation and Video Imaging of Single Microsphere Formation. Real-time recordings of the formation of single FA, RIF, and FA-RIF coloaded PLGA microspheres were captured using a micropipet manipulation system as described in detail elsewhere.[31] Briefly, single droplets of FA/RIF/PLGA solution in DCM were formed at the tip of a 5 μm diameter borosilicate glass micropipet into a solution of 0.025 M SDS. Once the emerging droplet reached

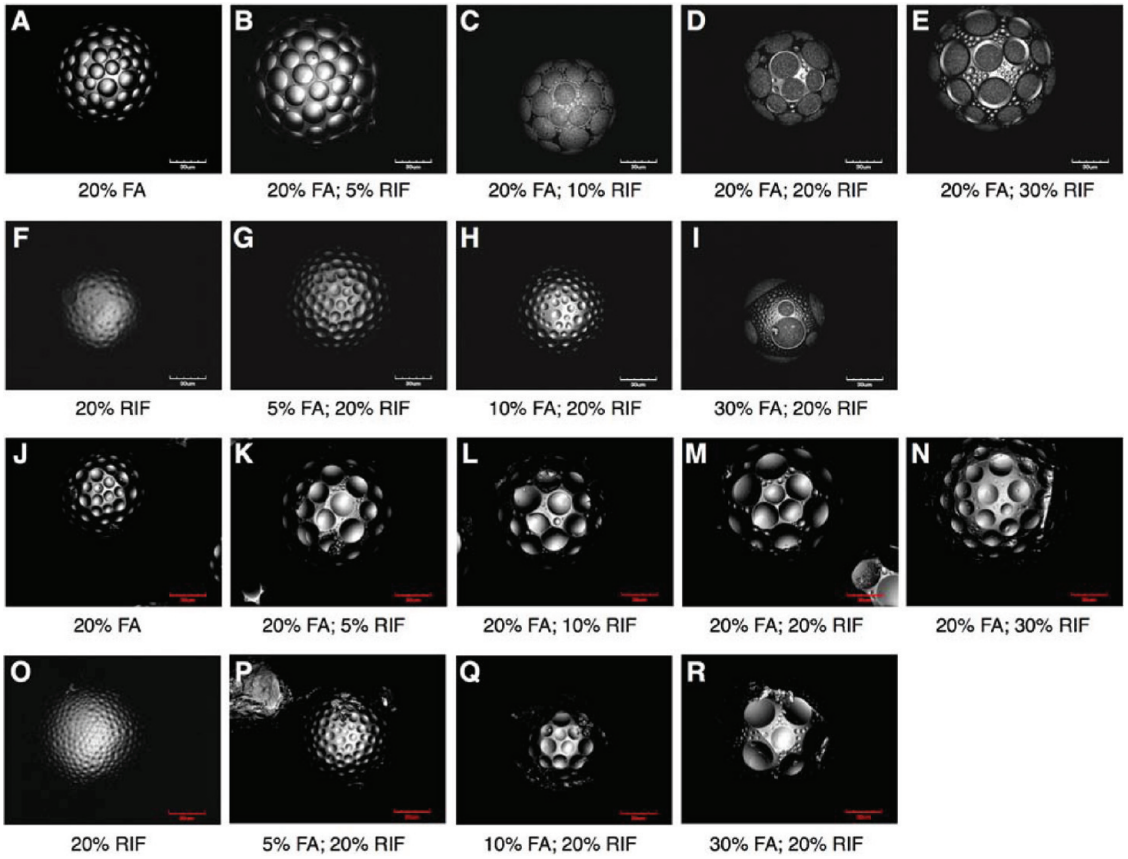

Figure 1. Laser confocal micrographs illustrating the detailed surface morphology of microspheres containing FA and RIF before (**A**–**I**) and after (**J**–**R**) 7 day release in PBS (pH 7.4; containing 0.1 mg/mL ascorbic acid) at 37 °C.

the desired diameter (~100 μm), the micropipet manipulator was gently tapped to release the solution droplet, which was either allowed to fall to the bottom of the chamber or immediately recaptured on the end of the micropipet. The droplet was observed and the image digitally recorded as the DCM diffused into the surrounding aqueous phase, resulting in a solidified microsphere. The experimental setup includes an inverted optical microscope (Diaphot 200; Nikon, Melville, NY, USA) with a 40× or an oil-immersion 100× objective lens, a micropipet manipulation system, and video capturing equipment. The camera (Pike F-100B; Allied Vision Technologies, Stadtroda, DE) was controlled via a computer with StreamPix software (Norpix, Montreal, QC, CA) and the captured video analyzed using ImageJ software (National Institutes of Health). The chamber used with the 40× objective lens was a standard glass cuvette (2-mm path length).[31,32] For experiments with the oil-immersion objective, the chamber was formed from coverslips (22 × 30 mm) and cut glass microscope slides.[33] Coverslips were affixed to the top and bottom of the glass slide pieces with vacuum grease to create a chamber with final dimensions of approximately 22 × 25 × 2 mm, which was open on two sides.

Mass Composition Calculations for Single Microdroplets. The solute concentration during phase separation was calculated as a function of time and was based on the volume change of the single droplet. The initial solution density, ρ_i, and total solute concentration (i.e., drug + PLGA), c_i, were calculated from the weight fraction (w) of each component assuming no volume change on mixing, where

$$\frac{1}{\rho_i} = \frac{w_{DCM}}{\rho_{DCM}} + \frac{w_{PLGA}}{\rho_{PLGA}} + \frac{w_{DRUG}}{\rho_{DRUG}} \tag{3}$$

and

$$c_i = (w_{PLGA} + w_{DRUG})\rho_i \tag{4}$$

In all calculations, it was assumed that neither drug nor polymer dissolved into the surrounding aqueous phase, and therefore, the solute mass in the droplet remained constant. The solute concentration was then calculated as a function of time based on the volume change of the droplet according to $c = (c_i v_i)/v$, where v_i is the initial volume of the droplet and v is the volume of the droplet as a function of time. The solute concentration at the time of phase separation was calculated according to the diameter of the droplet when the first signs of phase separation were visible (as indicated in Figure 5A). To calculate this in terms of the solute mass fraction, the mass of DCM in the droplet was also calculated as a function of time by subtracting the mass lost from the initial DCM mass, $m_{DCM} = m_{i,DCM} - m_{lost,DCM}$. The initial mass is given by $m_{i,DCM} = w_{i,DCM} v_i \rho_i$, and the mass lost is given by $m_{lost,DCM} = (v_i - v)\rho_{DCM}$. The mass fraction of total solute, $w_{PLGA+DRUG}$, can then be calculated according to the following:

$$w_{PLGA+DRUG} = \frac{\text{solute mass}}{\text{solute mass} + \text{DCM mass}} = \frac{c_i v_i}{c_i v_i + w_{i,DCM} v_i \rho_i - (v_i - v)\rho_{DCM}} \tag{5}$$

dx.doi.org/10.1021/mp300099f | Mol. Pharmaceutics 2012, 9, 1489–1501

Table 1. Summary of the Thermal and Physical Characteristics of FA- and RIF-Loaded PLGA (50:50) Microspheres Formed by Solvent Evaporation[a]

	thermal characteristics			physical characteristics		
microsphere formulation	T_r (°C)[b]	ΔH_r (J/g)[c]	T_g (°C)[d]	mean diameter (μm) (PDI)[e]	EE_{FA} (%)[f]	EE_{RIF} (%)[f]
20% FA; 0% RIF	56.8 ± 0.17	7.9 ± 1.1	117.9 ± 0.06	71.5 (0.69)	82.0 ± 7.4	
20% FA; 5% RIF	57.0 ± 0.15	6.7 ± 1.0	125.1 ± 0.14	93.4 (0.76)	85.3 ± 5.1	87.8 ± 3.3
20% FA; 10% RIF	57.1 ± 0.32	6.2 ± 1.2	129.7 ± 0.27	87.4 (0.9)	90.7 ± 6.0	85.3 ± 4.9
20% FA; 20% RIF	57.4 ± 0.18	6.5 ± 0.5	137.0 ± 0.25	99.9 (1.22)	86.9 ± 3.0	85.3 ± 2.6
20% FA; 30% RIF	57.9 ± 0.33	4.7 ± 0.5	140.6 ± 0.16	101.6 (0.79)	84.2 ± 2.5	85.1 ± 1.8
30% FA; 20% RIF	57.5 ± 0.11	4.6 ± 0.2	131.3 ± 0.34	94.2 (0.75)	96.7 ± 1.4	87.6 ± 1.9
10% FA; 20% RIF	57.2 ± 0.46	6.4 ± 0.9	146.7 ± 1.56	121.1 (1.54)	84.3 ± 7.0	74.4 ± 1.9
5% FA; 20% RIF	56.2 ± 0.16	6.6 ± 0.2	150.9 ± 0.73	112.3 (0.9)	89.8 ± 4.4	79.6 ± 0.9
0% FA; 20% RIF	55.2 ± 0.83	6.5 ± 0.6	159.22 ± 1.7	131.6 (1.2)		75.9 ± 2.3

[a]Results are expressed as the mean ± S.D. $n = 3$. [b]T_r = Enthalpy of relaxation temperature. The peak temperature of the first endothermic transition in the first heating cycle. [c]ΔH_r = Enthalpy of relaxation. Integration of the first endothermic transition in the first heating cycle. [d]T_g = Glass transition temperature for the mono- or coloaded drugs. The midpoint of the heat capacity change in the first heating cycle. [e]PDI = Polydispersity index. Measured by the span, according to eq 1. A smaller span indicates a narrow size distribution. [f]EE = Encapsulation efficiency. Recovered drug expressed as a percentage of the theoretical drug loading.

Solute mass fractions were calculated assuming the following densities: ρ_{PLGA} = 1.34 g/mL; ρ_{DCM} = 1.33 g/mL; ρ_{RIF} = 1.34 g/mL; ρ_{FA} = 1.16 g/mL.

FA, RIF, and PLGA Compatibility Calculations. The compatibility (i.e., constant volume internal energy of mixing) between FA and RIF and PLGA was calculated by the Hildebrand–Scatchard equation and the enthalpy of mixing (ΔH_M) as determined by Hildebrand. The Hildebrand–Scatchard equation is expressed as follows:

$$\chi_{sp} = (\delta_{drug} - \delta_{PLGA})^2 \frac{V}{RT} \tag{6}$$

where χ_{sp} is the Flory–Huggins interaction parameter, δ_{drug} is the solubility parameter for either FA (δ_{FA}) or RIF (δ_{RIF}), and δ_{PLGA} is the solubility parameter for PLGA; R is the gas constant; T is the temperature in Kelvin; and V is the molar volume of the added drug as calculated by the group contribution method.[34] For this evaluation, values for δ_{FA} and δ_{RIF} were calculated using the additive group contribution method described by van Krevelen,[35] where each solubility parameter is the sum of the dispersion (δ_d), polar (δ_d), and hydrogen bonding components (δ_d) such that

$$\delta_{drug}^2 = \delta_d^2 + \delta_p^2 + \delta_h^2 \tag{7}$$

and

$$\delta_{PLGA}^2 = \delta_d^2 + \delta_p^2 + \delta_h^2 \tag{8}$$

Each component was calculated according to the following equations:

$$\delta_d = \sum \frac{F_{di}}{V} \tag{9}$$

$$\delta_p = \frac{(\sum F_{pi}^2)^{1/2}}{V} \tag{10}$$

$$\delta_h = \left(\sum \frac{E_{hi}}{V}\right)^{1/2} \tag{11}$$

where F_{di} is the molar dispersion constant, F_{pi} the polar attraction constant, and E_{hi} the hydrogen bonding energy. All values were found in tables published by van Krevelen.[35] The solubility parameter for the polymer (δ_{PLGA}) was taken from previously published literature values.[36]

The calculation of ΔH_M was done using the following equation:

$$\Delta H_M = \phi_{Drug}\phi_{PLGA}[(\delta_{d,Drug} - \delta_{d,PLGA})^2 + (\delta_{p,Drug} - \delta_{p,PLGA})^2 + (\delta_{h,Drug} - \delta_{h,PLGA})^2] \tag{12}$$

where ϕ_{Drug} and ϕ_{PLGA} are the molar volume fractions of the drug (FA or RIF) and PLGA, respectively, based on the molar volumes calculated by the group contribution method.[35]

RESULTS

FA, RIF, and FA-RIF Coloaded PLGA (50:50) Microspheres. As shown in Figure 1A, pure FA loaded PLGA microspheres (at 20% loading) showed regular spherical protrusions. Microspheres containing 20% RIF were characterized by small concave surface dimples (Figure 1F). For the mixed systems, microspheres containing 20% (*w/w*) FA with increasing RIF coloading (Figure 1B–E) displayed uniform microdomains that appeared as spherical surface protrusions with distinct boundaries. The interstitial surface space between these spherical protrusions showed a dimpled appearance characteristic of pure RIF. For RIF-loaded microspheres (20% *w/w*) with increasing amounts of FA, the dimpled morphology became more pronounced with FA addition up to 10% FA (*w/w*), but once the FA loading reached or exceeded 20% (*w/w*), spherical protrusions appeared, reminiscent of the 20% FA system with added RIF. Detailed surface morphologies for both initial and drug-released released microspheres are shown in Figure 1.

FA-loaded microspheres showed an increase in mean diameter with the coloading of RIF in a dose dependent manner with mean diameters of 71.5 μm for FA monoloaded microspheres increasing to 93.4 μm, 87.4 μm, 99.9 μm, and 101.6 μm, for RIF coloadings of 5, 10, 20, and 30% (*w/w*), respectively. In contrast, RIF-loaded microspheres demonstrated a decrease in mean diameter with FA coloading, with mean diameters of 131.6 μm for RIF monoloaded microspheres decreasing to 112.3 μm, 121.1 μm, and 94.2 μm, for FA coloadings of 5, 10, and 30% (*w/w*), respectively. Formulations were characterized by high FA encapsulation efficiency ranging

from approximately 82% to 97%, with no apparent dependence on drug loading. RIF encapsulation was slightly lower than that of FA, ranging from approximately 75% to 87%, with higher RIF loadings achieved once FA theoretical loadings were ≥20% (*w/w*). The physical characteristics of the microspheres are summarized in Table 1.

Raman Spectroscopy Analysis of FA and RIF Coloaded PLGA (50:50) Microspheres. To determine the nature of the various surface microdomains shown in Figure 1, Raman surface mapping of FA and RIF coloaded PLGA microspheres was performed using Raman shift data between 1800 cm^{-1} and 700 cm^{-1}. Unfortunately, the high scattering intensity of RIF precluded the ability to map the microsphere surface for actual drug localization; however, we were able to map the surface of the coloaded microsphere for the PLGA distribution. Figure 2 shows that the PLGA signal is limited to

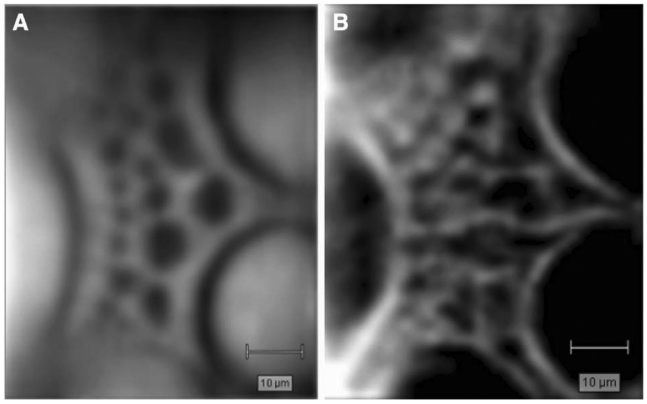

Figure 2. Raman confocal images of 20% (w/w) FA and 20% (w/w) RIF coloaded into PLGA microspheres. (A) Confocal image illustrating the microsphere morphology. (B) Chemical map showing the variation in distribution of PLGA. Light areas show the presence of PLGA and dark areas the absence.

the areas around the surface microdomains, suggesting that the drugs are localized within the protruding and dimpled microdomains.

XRPD Analysis of FA, RIF, and Coloaded PLGA (50:50) Microspheres. Representative XRPD patterns of the drug-loaded microspheres, and physical mixtures of FA, RIF, and PLGA are shown in Figure S1 of the Supporting Information. There was no evidence of crystallinity in any of the microsphere formulations, as illustrated by a characteristic amorphous halo in the XRPD pattern.

Thermal Characterization of FA, RIF, and FA-RIF Coloaded PLGA (50:50) Microspheres and Cosolidified Drugs. Representative DSC scans of FA, RIF, and FA-RIF coloaded PLGA microspheres are shown in Figure S2 of the Supporting Information and summarized in Table 1. All formulations displayed an enthalpy of relaxation endotherm (T_r) at approximately 57 °C, which was associated with the T_g of PLGA; the second heating cycle, after quench cooling, was also characterized by a single T_g between 40 and 43 °C, characteristic of PLGA (Table 1). A glass transition (T_g) between 116 and 150 °C was also observed on the first heating cycle, and this was characteristic of a thermal transition attributed to the drug(s). For the 20% FA in PLGA, the T_g was at 117.9 °C ± 0.06 °C, and for 20% RIF in PLGA, the T_g was at 159.22 ± 1.7 °C. As expected from a reciprocal combination of the mixtures, the measured T_g for the first heating cycle was dependent on the FA and RIF content of the coloaded microspheres. That is, the inclusion of RIF in 20% FA loaded microspheres resulted in a concentration-dependent increase in T_g. Conversely, the inclusion of FA content in 20% RIF microspheres resulted in a concentration-dependent decrease in the T_g.

Thermal analysis of FA and RIF and FA-RIF mixtures cosolidified by solvent evaporation from DCM in the absence of PLGA showed single observable T_g values covering the range between the two pure materials. The T_g values for cosolidified drug and microspheres are illustrated in Figure 3, plotted along with the calculated T_g of a miscible blend of FA-RIF, determined by the Fox equation.

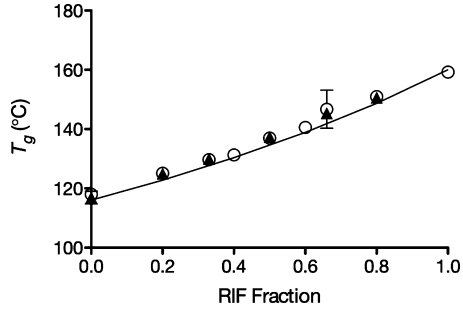

Figure 3. Effect of blending increasing amounts of RIF with FA on the glass transition temperature (T_g) of the blend from (○) 20% (*w/w*) FA-loaded PLGA microspheres prepared by single O/W emulsion and solvent evaporation, and (▲) the antibiotics cosolidified from DCM with no polymer present. The solid reciprocal line represents theoretical values based on the Fox equation. Each data point represents the mean ± SD of n = 3 scans.

Micromanipulation and Analysis of Single Microsphere Formation. Using a micropipet technique, PLGA microsphere formation was observed in real time for solutions of 20, 40, and 60% (*w/w*) drug/PLGA content for FA, RIF, and coloaded (FA/RIF; 1:1) microspheres. All solutions had a starting composition of ∼10% (*w/v*) of total solids (drug and polymer) in DCM. Representative videomicrographs of 20% (*w/w*) FA and RIF monoloaded and 20% FA/RIF (1:1) coloaded PLGA microspheres are shown in Figure 4. Note that, to see the details of microstructure and phase separations, a higher magnification oil immersion lens was used to obtain the images in Figure 4. This necessitated studying smaller microspheres than those that provided the data in Figure 5, and thus, the time lines for Figures 4 and 5 do not match, as the relatively small microspheres of Figure 4 lose solvent and reach the phase precipitation faster than the larger population shown in Figure 5.

All formulations were characterized by FA or RIF phase-separation events. For 20% (*w/w*) FA-loaded microspheres (Figure 4A), the first phase separation of FA-rich droplets occurred very rapidly (see Figure 4A; 3 and 8 s). Since water is not very soluble in DCM, it would seem that this is a FA-DCM phase in the PLGA/DCM droplet. In the absence of FA, there are no water inclusions, but the aqueous solubility of FA is 5.2 × 10^{-3} g/L, and so we cannot completely rule out that this FA-rich phase does not contain any water. With further loss of DCM solvent and shrinking of the microdroplet volume, these FA-rich microdroplets within the forming microsphere coalesced to form larger microdroplets. As the microsphere approached the viscous boundary, the viscosity of the forming

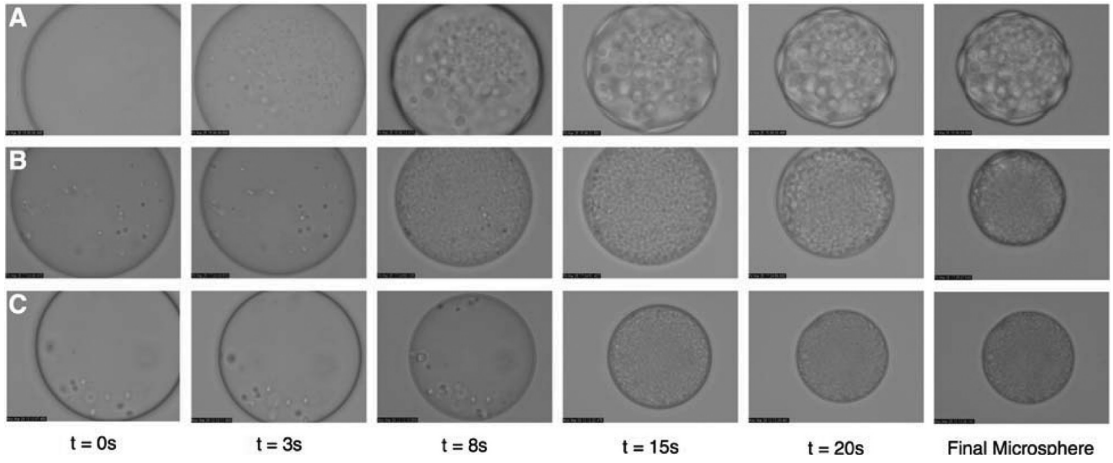

Figure 4. Time lapsed video images (FOV = 58 μm × 43 μm) illustrating the formation of PLGA (50:50) microspheres containing (A) 20% (*w*/*w*) FA, (B) 20% (*w*/*w*) FA:RIF (1:1 as 10%:10%), and (C) 20% (*w*/*w*) RIF. All microspheres were created with an initial polymer and drug concentration of 10% (*w*/*v*). The detailed surface morphologies of the corresponding microspheres by surface SEM are depicted in Figure 1.

microsphere increased (Brownian motion of internal particles slowed dramatically) and some of the FA-rich droplets in the interior of the solidifying microsphere became kinetically trapped within the bulk of the microsphere, while ones closest to the surface condensed out at the surface (see Figure 4A; ∼15 s). Thus, what appeared to be the FA-rich phase was excluded from the PLGA matrix and localized as microdomains at the surface of the solidifying microsphere (Figure 4A; 20 s). These data are very similar to, and confirm, our previous observations for FA/PLGA microsphere formation.[8]

For the 20% (*w*/*w*) RIF-loaded microspheres (Figure 4C), small water inclusions can sometimes be incorporated into the droplet as it emerges from the micropipet (due to differential wetting and displacement of the water film on the glass). The RIF phase separates from PLGA (Figure 4C) considerably later than FA does in a microsphere of comparable (60 μm) size. RIF is more water-soluble in an aqueous phase (4.13×10^{-2} g/L) and might be expected to imbibe more water than FA into the PLGA microsphere, and therefore, we cannot rule out that this RIF-rich phase contains some water. As shown in Figure 4C, the RIF-rich microdroplets did not appear to coalesce very much, which might be explained by the fact that, by the time the RIF phase separates as small droplets, the viscosity of the polymer droplet was high enough to prevent much Brownian motion and RIF-rich droplet motion, at a relative droplet volume of 0.194 ± 0.000, which corresponds to a solute mass percent of 39.7 ± 0.1%. Thus, the separation of RIF was much later in the solidification process than the separation of FA in the FA-loaded formulation. In this monoloaded system, what appeared to be the phase-separation of drug-rich microdomains occurred much closer to the VB (relative droplet volume of 0.109 ± 0.001), as shown in Figure 4C, and the drug was more well encapsulated throughout the microsphere.

In the coloaded formulation (Figure 4B), the phase separation of both drugs occurred in a single event at a relative droplet volume of 0.251 ± 0.002, which corresponds to a solute mass percent of 31.1 ± 0.3%, midway between the two monoloaded formulations. The phase separation was also consistent with each drug's behavior in that some droplets were retained in the interior, similar to RIF, while larger domains precipitated at the microsphere surface, characteristic of FA phase separation.

The data from the micromanipulation experiments on larger microdroplets (95.9 ± 3.0 μm) were then used to plot the changes in relative microsphere volume during microsphere solidification for microspheres composed of FA, RIF, or FA-RIF (1:1), in PLGA over the course of solidification (Figure 5A). The mass composition of drug, PLGA, and DCM at the point of phase separation was quantified according to eqs 3 to 5. The viscosity boundary (VB), defined as the onset of polymer gelation,[22] is indicated at a relative droplet volume of 0.095 ± 0.044, as shown by the inflection in Figure 5A. Consistent with the images in Figure 4, the slightly larger population of microspheres showed the same drug and drug mixture phase separation in relation to the viscous boundary (FA < FA-RIF < RIF).

The data from the micromanipulation experiments were then used to construct a ternary phase diagram to better illustrate the solute composition of the mono- and coloaded microspheres at the point of phase separation (Figure 5B). The apex entitled "DRUG" represents FA, RIF, or FA-RIF (1:1). Each formulation, FA, RIF, and FA-RIF (1:1), was evaluated at 20%, 40%, and 60% (*w*/*w*) relative to PLGA, to evaluate the role of drug load on the phase separation. This figure illustrates that the phase separation of FA occurred much earlier in the solidification process than that of RIF. Furthermore, when both FA and RIF were encapsulated (1:1), the phase boundary of the coloaded formulation (represented as the "drug" apex on the diagram) was between the two monoloaded formulations.

Drug−Polymer Compatibility. The Hildebrand−Scatchard equation (eq 6) was used to calculate the Flory−Huggins interaction parameter (χ_{sp}) for the binary mixtures of FA or RIF and PLGA, using the group contribution method. The partial solubility parameters were also used to calculate the enthalpy of mixing (ΔH_M) of the binary mixtures using eq 12. The total solubility parameters (δ_{drug} or δ_{PLGA}), molar volume (V), χ_{sp}, and ΔH_M values are shown in Table 2.

***In Vitro* Release Profiles of FA and RIF from Mono- and Dual-Loaded PLGA (50:50) Microspheres.** The *in vitro* release profiles of FA and RIF are plotted in Figure 6. All formulations containing 20% (*w*/*w*) FA (±RIF) were characterized by an initial burst of FA (Figure 6A) and RIF (Figure 6B) over 1 h, with no further FA release and a moderate release of RIF over 7 days, with the exception of microspheres containing 30% (*w*/*w*) RIF, which showed a

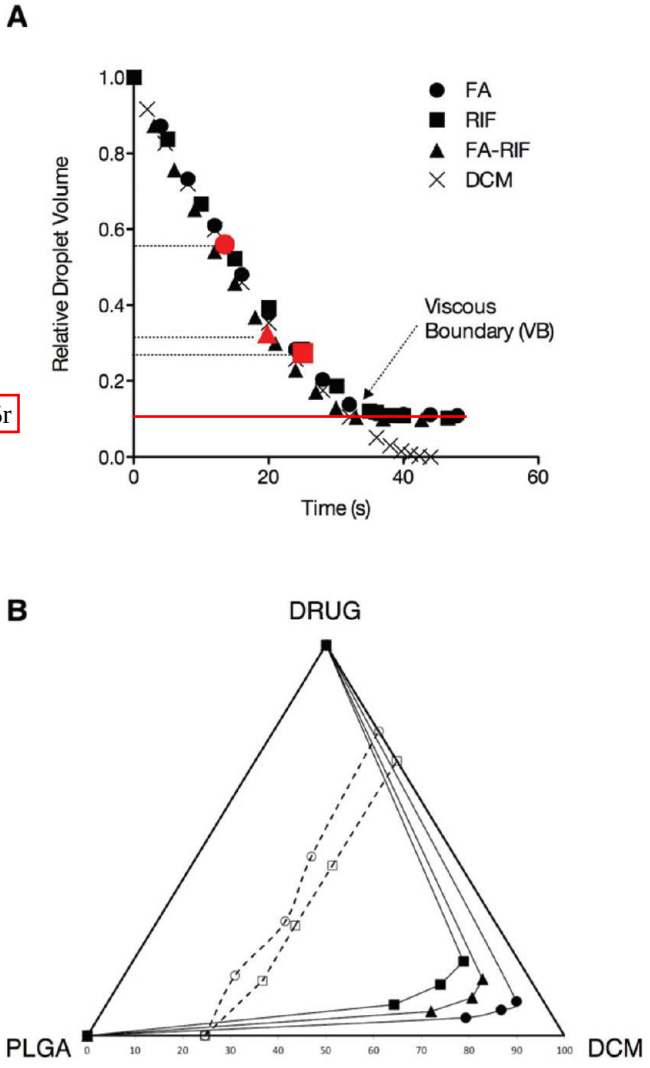

Figure 5. (A) Representative plot of the changes in relative microsphere volume during microsphere solidification for microspheres composed of FA (●), RIF (■), or FA-RIF (1:1) (▲), in PLGA as determined by micropipet experiments. The droplet volume at the point of phase separation is shown in red for FA (red circles), RIF (red squares), and FA-RIF (red triangles). (B) Ternary phase diagram illustrating the composition at the point of drug phase separation for microspheres containing FA (●), RIF (■), and FA-RIF (▲). All compositions were calculated using eqs 3–5 and are given in mass %. The dotted lines represent the microsphere composition at the viscous boundary for FA (○) or RIF (□), which is shown as the inflection point in part A.

Table 2. FA, RIF, and PLGA Compatibility Data

microsphere component	δ_{drug} or δ_{PLGA}[a] ($MPa^{1/2}$)	V[b] ($cm^3 \cdot mol^{-1}$)	χ_{sp}[c,d]	ΔH_M[e]
FA	21.1	443.4	0.72	9.47
RIF	24.6	591.2	0.55	3.57
PLGA(50:50)[e]	23.1	47.7		

[a] δ_{drug} or δ_{PLGA} = total solubility parameter for the drugs and polymer as calculated from eq 7 or 8. [b] V = molar volume of the drug or polymer, calculated according to ref 34. [c] χ_{sp} = Flory–Huggins interaction parameter calculated from eq 6. [c] ΔH_M = enthalpy of mixing calculated from eq 12. [d] Critical solubility value = χ_{sp} value for solubility limits; insoluble > 0.5 > soluble.[40] [e] The δ_{PLGA} and V of PLGA (50:50) were taken from literature values.[36]

moderate controlled-release over 7 days. In contrast, formulations containing 20% (*w*/*w*) RIF (±FA) did not release FA (Figure 6C) and only released very low quantities of RIF (<5%; Figure 6D). It was not until a 20% (*w*/*w*) coloading of FA that any appreciable release of FA or RIF was observed (Figure 6A and B). Figure 1J–R shows the detailed surface morphology of microspheres following 7 days release in PBS (pH 7.4), revealing the disappearance of the spherical protrusions on the microsphere surface.

■ DISCUSSION

In this investigation, we explored the ternary phase separation behavior and miscibility characteristics of FA and RIF loaded into PLGA microspheres. This exploration was mainly based on observations of interesting morphological features in the mono- and coloaded PLGA microspheres. Although a small number of reports have shown microspheres with similar features,[8−10,14,15] there have been no attempts to explain the phase phenomena underlying these observations. Of particular importance was the ability to visualize microscopic images of the whole process of microsphere formation from single PLGA–DCM–drug solution microdroplets using a micropipet technique.

Microsphere formation is a process of interface creation, mass transfer, and phase separation. It occurs in three distinct steps: (1) droplet formation into a second aqueous phase; (2) solvent removal into the aqueous solvent and solidification of the polymer and drug; (3) final drying to remove all solvent. Parameters that influence the diffusion of solvent from the dispersed phase and subsequent solidification of the polymer and the codissolved drugs are critical to the ultimate drug release profiles of the resulting microspheres. Understanding the mixing relations, mutual solubilities, and insolubilities of the components is essential for the rational design of controlled release. The processes governing the solidification of microspheres can be divided into three temporal states: (1) the solution state, (2) the gel state, and (3) the glassy state. In the solution state, the mass transfer of solvent to the continuous phase results in the liquid–liquid phase separation of a polymer-rich outer layer and a polymer-poor inner core, which has been termed binodal decomposition.[22] According to DeLuca, the polymer-rich liquid phase is composed of PLGA, organic solvent, and small amounts of encapsulated drug, while the polymer-poor liquid phase contains the majority of the encapsulated drug and solvent. This initial phase separation then is dependent on the relative polymer concentration in each phase and is the equilibrium between a concentrated polymer swollen by solvent, and solvent with a small amount of polymer dissolved. In stage 2, as the mass transfer of solvent continues from the polymer–drug dispersed phase, the droplet reaches a gelation point, where the polymer–drug solution becomes concentrated and more viscous. This point is termed the viscous boundary (VB) depicted earlier in Figure 5. The mass transfer of organic solvent out of the now gelatinous microsphere is slowed considerably at the VB, and the transport of molecular solvated drug or drug particles inside the microsphere is restrained. The drug–polymer droplets remain in the gel state until mass transfer is complete, when the droplets reach the third stage, the glassy state, and form the final solid-state microsphere. Drug can associate with polymer as a molecular level dispersion of drug within the polymer interstitial space (solid solution), or it could precipitate as distinct separate domains/clusters (forming a solid suspension), in which the drug particles may be crystalline or

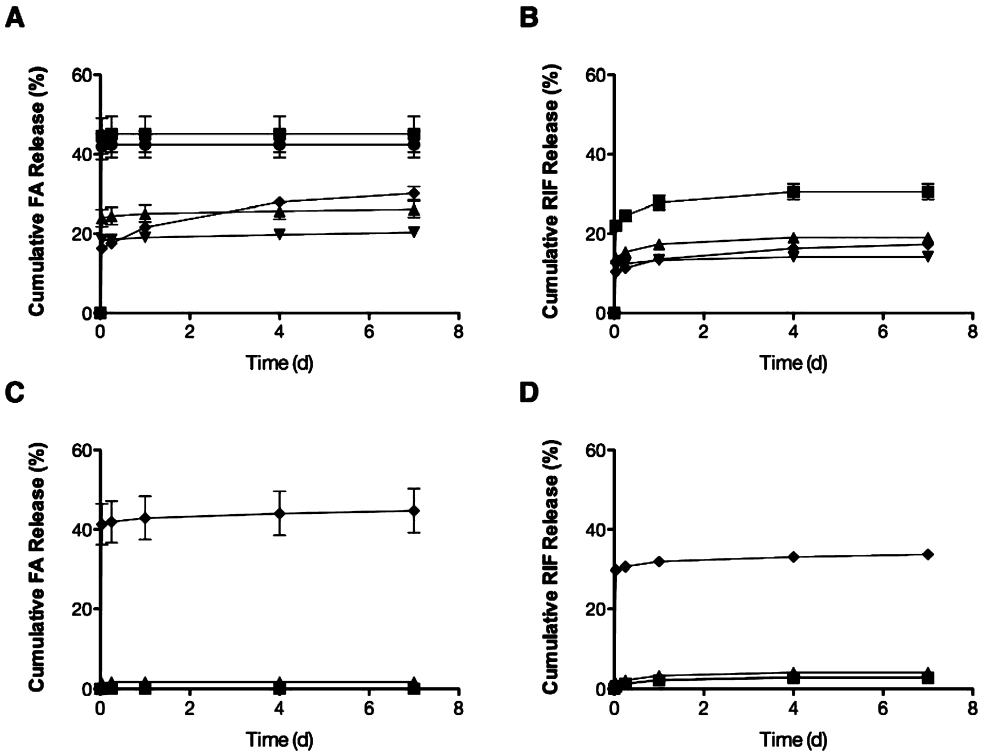

Figure 6. *In vitro* release profiles of FA and RIF from mono- and coloaded PLGA (50:50) microspheres performed in PBS (pH 7.4; containing 0.1 mg/mL ascorbic acid) at 37 °C. (A) FA release from 20% *(w/w)* FA-loaded PLGA containing (●) 0% RIF, (■) 5% RIF, (▲) 10% RIF, (♦) 20% RIF, and (♦) 30% RIF. (B) RIF release from 20% *(w/w)* FA-loaded PLGA microspheres containing (■) 5% RIF, (▲) 10% RIF, (▼) 20% RIF, and (♦) 30% RIF. (C) FA release from 20% *(w/w)* RIF-loaded PLGA microspheres containing (■) 5% FA, (▲) 10% FA, and (♦) 30% FA. (D) RIF release from 20% *(w/w)* RIF-loaded PLGA microspheres containing (●) 0% FA, (■) 5% FA, (▲) 10% FA, and (♦) 30% FA. $n = 3 \pm$ SD.

amorphous.[37] However, if the outer shell of the microsphere is sufficiently viscous, drug that is not molecularly dispersed (i.e., drug that exists as phase separated domains/clusters) cannot be efficiently transported into the outer layer, trapping it in this more concentrated polymer phase.

As shown in Figure 1A, monoloaded microspheres containing 20% FA displayed uniform, spherical surface protrusions with distinct boundaries on the microsphere surface. This morphology has been shown before by our group for FA-PLGA microspheres,[8] and similar morphologies have been shown for PLLA microspheres loaded with cyclosporine A,[9,10] as well as cellulose acetate films containing Vitamin E.[21] Similar spherical protrusions on the surface of polymer films and microspheres are therefore thought to be due to an insolubility of the drug in the polymer and the phase exclusion of drug-rich domains from the polymer matrix in PLGA, PLLA, and cellulose acetate. The fact that they are spherical indicates that they have a liquid origin, that is an immiscible liquid phase with a significant interfacial tension.

Microspheres containing 20% (*w/w*) RIF were characterized by small concave surface dimples (Figure 1F). These concave dimples increased in size with FA loading until the FA loading reached 20% (*w/w*), where spherical protrusions were once again visualized (Figure 1D). Similar concave dimpled morphologies have been shown for PLLA microspheres encapsulating the anticancer drug paclitaxel[14] and were attributed to solid−solid phase separation of drug from the polymer. It was suggested that the encapsulated drug was a principal component of the initially formed surface layer during microsphere hardening.[38] Therefore, it is likely that the dimpled morphology in microspheres with higher RIF loadings began as numerous small spherical domains, similar to what is seen with FA, as a result of RIF being a component of the highly viscous surface layer. However, due to the higher aqueous solubility of RIF, these domains undergo dissolution in the continuous phase during the microsphere hardening process, resulting in loss of phase-separated domains, forming concave dimples. Although we were unable to visually confirm this, the loss of surface associated drug may explain the lower encapsulation efficiency in the microspheres with higher RIF loadings. Nevertheless, the change from a dimpled morphology to one with spherical surface protrusions with increasing FA content suggests that, at higher loadings (i.e., 20%), the FA incompatibility in PLGA begins to determine the phase separation and is also promoted by the lower aqueous solubility of FA (5.2×10^{-3} g/L for FA compared to 4.13×10^{-2} g/L for RIF).

To further investigate the nature and composition of the phase-excluded microdomains, each microsphere formulation was subjected to XRPD and thermal analysis by DSC. XRPD patterns of each formulation were compared to XRPD patterns of physical mixtures of each drug with PLGA. All microsphere formulations were characterized by an amorphous halo, with no evidence of crystallinity in any formulation, suggesting that the drugs were present in the solid microsphere in the amorphous form. Thermal analysis supported this observation, as no melt endotherms were observed upon heating. All FA, RIF, and FA-RIF coloaded microspheres were characterized by an enthalpy of relaxation endotherm (T_r), attributed to PLGA, and a glass transition (T_g) at ∼45 °C on the second heating cycle after quench cooling (Figure S2 in the Supporting Information; second heating cycle not shown). The enthalpy of relaxation

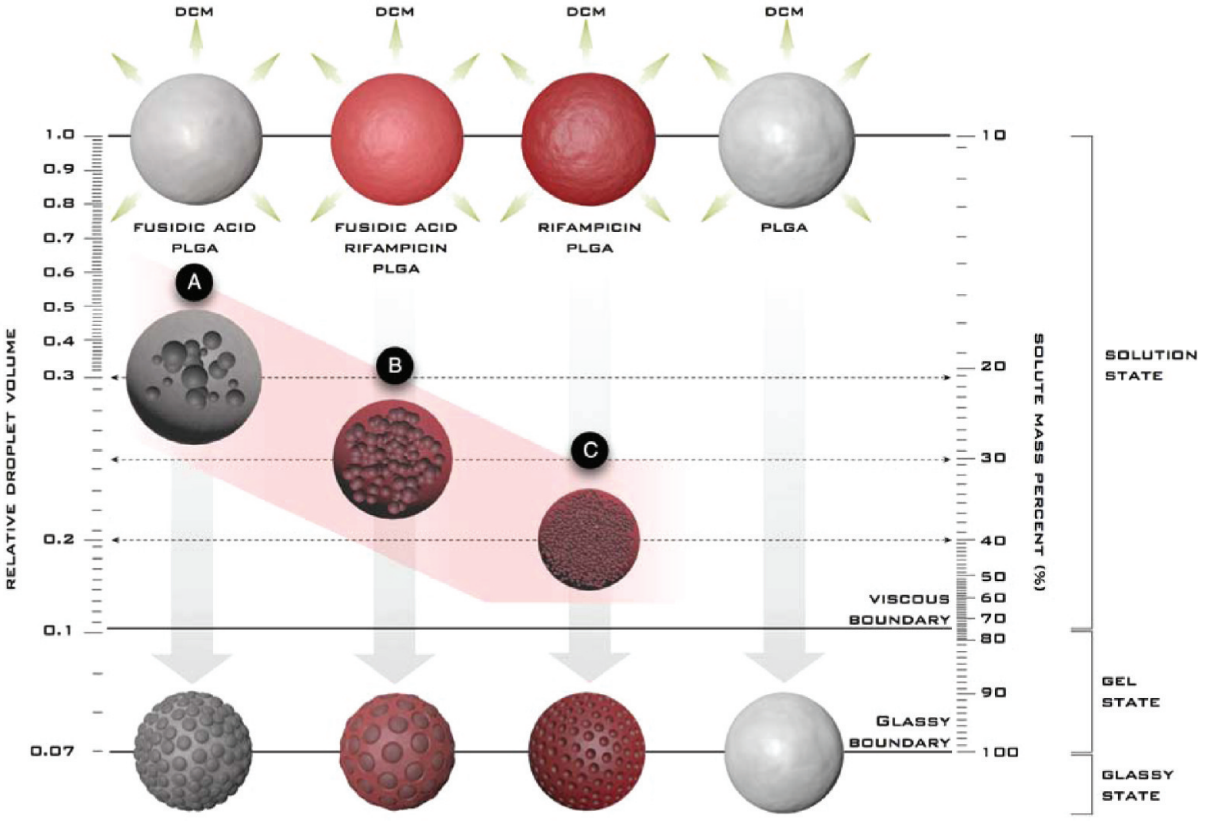

Figure 7. Schematic illustration of the phase separation of FA, RIF, and a combination of FA−RIF from PLGA in microspheres. Note: Images are to illustrate the morphologies involved and are not representative of the obvious volume changes, especially in the glassy state, where microspheres would be much smaller than illustrated. The pink shading represents the first signs of drug phase separation. As DCM diffuses out of the dispersed phase, (A) FA phase separates at a relative droplet volume of 0.311 ± 0.014. The early separation in the solution state at a relatively low solution viscosity allows for coalescence of FA-rich microdroplets within the microsphere interior. Convective currents drive the microdropets to the microsphere interface prior to final polymer gelation. The resulting microsphere is characterized by FA-rich microdomains localized to the surface of the microsphere. (B) In FA-RIF coloaded microspheres, the phase separation of both FA and RIF occurs at a relative droplet volume of 0.251 ± 0.002 due to the increased compatibility between RIF and PLGA. At this point, the solution still has a sufficiently low viscosity to allow for coalescence of microdroplets; the relative contribution of FA allows for surface exclusion of some drug-rich microdomains. The resulting morphology is characterized by larger, but fewer, surface domains. (C) RIF phase separates from PLGA at a relative droplet volume of 0.194 ± 0.000 due to increased RIF/PLGA compatibility. As this occurs closer to the VB, the solution viscosity is relatively large and there is limited coalescence of individual phase separated RIF droplets. RIF remains largely localized to the bulk of the microsphere. Surface exposed drug solubilizes in the continuous phase during gelation (higher RIF aqueous solubility), and the resulting morphology is characterized by small surface dimples.

occurs concurrently with the polymer T_g, and is a result of short-range order within the glassy regions of the polymer that occurs during aging or processing.[38] Quenching the sample (i.e., removing the thermal history) eliminates the enthalpy of relaxation, and a single T_g, characteristic of PLGA, is observed at ∼45 °C on the second heating cycle. Since there was no influence of drug loading on the T_g of PLGA, this suggests that both drugs have extremely limited solubility in PLGA and completely phase separate from the polymer. Accompanying the polymer transition, there was only one other observable thermal event on the first heating cycle, a T_g ranging from ∼116 to 150 °C . This single T_g, well above the T_g of PLGA, suggests that the amorphous phase-separated microdomains contained both FA and RIF as a single miscible glass. To evaluate whether PLGA has an influence on the miscibility of FA and RIF, the drugs were cosolidified by solvent evaporation from DCM in the absence of PLGA. DSC analysis on the drug cosolidified from DCM showed a single T_g spanning the same range observed in the PLGA microspheres, with a dependence on the weight contribution of RIF (Figure 3). All measurements from microspheres and cosolidification experiments closely matched the theoretical calculations predicted by the Fox equation. Thus, we suggest that FA and RIF are miscible in all proportions, and the single thermal event in microspheres and cosolidified drugs indicated that both FA and RIF were colocalized as an amorphous solid in spherical microdomains on the surface and within the bulk of the PLGA microspheres.

Surface mapping of coloaded microspheres using high spatial resolution Raman spectroscopy was employed to confirm that the phase separated microdomains on the surface of the microsphere were composed of colocalized FA and RIF. Unfortunately, RIF produced very high fluorescence and scattered light at a magnitude of ∼100× and ∼30× those of FA and PLGA, respectively, which did not allow useful Raman information to be collected on the distribution of RIF. It is likely that a resonant effect is occurring to amplify the Raman signal, which typically happens when the virtual energy level of the input laser coincides with the electronic state of the molecule. However, we were able to map the surface for PLGA distribution. As shown in Figure 2, the PLGA distribution is confined to the areas surrounding the spherical microdomains, and not within them (light areas show the presence, dark areas

the absence of PLGA). Hence, this provides additional evidence that the microdomains observed in the PLGA microspheres were composed of both FA and RIF as a single, amorphous microphase-separated solid.

The molecular solubilization of a drug in a polymeric carrier is largely determined by the compatibility between these two components. That is, for the drug to remain dissolved in the polymer, the adhesion forces (i.e., dispersion, polar, and hydrogen bonding forces) must be greater between polymer and drug molecules than between drug molecules. In the case of microsphere formation, if the drug and polymer are not sufficiently compatible, the drug molecules will associate into localized regions in the solidifying microsphere until saturation is reached, at which time the drug will become insoluble in the polymer and phase separate.[39] Thermodynamically, the ability of two components to form miscible blends requires favorable intermolecular interactions between the two components. Drug/polymer compatibility and miscibility can be quantified by determining the Flory–Huggins interaction parameter, either experimentally, by methods such as melting point depression or ellipsometric measurements, or through calculating the total Hildebrand solubility parameters (and subsequent χ_{sp} calculations) and the enthalpies of mixing (ΔH_M). The calculated Flory–Huggins interaction parameters and enthalpies of mixing both predicted that neither FA nor RIF would have complete solubility in PLGA (χ_{sp} value for solubility limits; insoluble > 0.5 > soluble[40]). However, our calculations do show that RIF is predicted to have higher compatibility with PLGA compared to FA (as demonstrated by the lower χ_{sp} and ΔH_M values) (Table 2). Therefore, we suggest that the formation of phase-separated, drug-rich microdomains and the time at which this phenomenon occurs is regulated by the absolute solubility of each drug in PLGA.

Micromanipulation techniques were used to visualize and characterize the phase separation of FA and RIF from PLGA microspheres. Real-time video images were temporally recorded from the solution phase of microsphere formation until they passed the viscous boundary and reached the gel phase. Representative videomicrographs in Figure 4 illustrate that both FA and RIF phase separate from PLGA in all formulations. Analysis of the real-time videos of microsphere formation allows for quantification of microdroplet composition at the point of phase separation. Figure 7 is a schematic representation of the stages of phase separation for mono- and coloaded PLGA microspheres compared to solidification of control PLGA microspheres. The phase separation of FA occurs very early during the solution state (relative droplet volume = 0.311 ± 0.014 for 20% FA) when the microsphere is still fluid (Figure 7; point A). The phase separation results in the coalescence of FA-rich microdroplets in the polymer-poor microsphere interior, where convective currents within the microsphere (from the mass transfer of solvent from the core) exclude them to the organic–aqueous phase boundary at the microsphere surface. Once the microsphere undergoes gelation (i.e., passes the VB), the microdroplets are no longer able to coalesce and are seen as smaller microdomains localized to the microsphere bulk. On the other hand, the phase separation of RIF (20% loading) occurs much closer to the gelation point, at a relative droplet volume of 0.194 ± 0.000, and it supports the higher compatibility in PLGA (as demonstrated by the lower χ_{sp} and ΔH_M values) (Figure 7; point C). Interestingly though, the microsphere has still not reached the VB and remains fluid, yet there is no visible convection within the forming microsphere, and the phase separated RIF-rich microdomains are not excluded to the surface of the forming microsphere. When coloaded, the phase separation of FA and RIF occurs as a single event, rather than an early phase separation of FA followed by the later phase separation of RIF. This event is governed by the compatibility of the FA-RIF mixture in PLGA, and it happens intermediate between FA and RIF phase separation (relative droplet volume = 0.251 ± 0.002) (Figure 7; point B). During this phase separation, there is still sufficient fluidity in the microsphere to allow for some surface exclusion; however, the majority of the separated drug mixture remains within the microsphere bulk. It is likely that RIF is altering the FA partitioning through an increased miscibility of FA in the solvent-rich RIF phase. However, the incompatibility of RIF with PLGA precludes complete compatibility in the ternary mixture containing FA, RIF, and PLGA. Kang et al. demonstrated a similar phenomenon using a two-phase polymer system composed of binary mixtures of PLGA and PEG, to which paclitaxel (PTX) was incorporated.[41] In this investigation, the authors show that PTX preferentially partitioned into the PEG domains in films containing up to 20% (*w*/*w*) PEG in PLGA. The formulation presented as a two-phase system, where the interactions between PTX and PEG were sufficient to prevent PEG crystallization, forming an amorphous solid solution of PTX in PEG, dispersed in an amorphous PLGA matrix.[41] Therefore, we suggest that FA preferentially partitions into the solvent-rich RIF phase during microsphere formation. At the solubility limit of RIF in PLGA, both drugs phase separate as a single amorphous phase with a distribution dependent on the relative contribution of FA.

In vitro release of FA and RIF from mono- and coloaded microspheres was almost completely dependent on the surface phase separation of drug-rich spherical domains (Figure 6). Where release was achieved, it was characterized exclusively by a large initial burst phase of release, with minimal release thereafter. The burst release was found to be due to the dissolution of the surface microdomains, as seen in Figure 1J–R, where the microdomains are absent following 7 day release in PBS. A similar effect has been observed with the encapsulation of Vitamin E in cellulose acetate films, where the release of Vitamin E was characterized exclusively by a burst release and dissolution of phase-separated surface domains.[21] These data indicate that the release of drug over 7 days is limited to microspheres where there are surface microdomains, and that release is almost entirely attributed to the dissolution of these spherical drug-rich reservoirs. In addition, for microspheres with higher loadings of RIF, there was little surface deposition of drugs, resulting in minimal burst release of both FA and RIF. This inverse relationship suggested that the coloading of RIF in the FA microspheres resulted in the drug remaining trapped in the interior, giving a limited drug exclusion to the microsphere surface and, hence, a reduced burst drug release.

CONCLUSIONS

In a polymeric drug delivery system, the compatibility of the drug (or mixture, in this case) with the encapsulating polymer will determine the drug deposition in the resulting formulation. Drugs may exist as molecular dispersions in the polymer interstitial space, or phase separated into microdomains, which occupy large voids in the polymer matrix. Detailed surface analysis of FA, RIF, and FA-RIF coloaded PLGA microspheres by confocal microscopy, Raman spectroscopy, real-time video

imaging of microsphere formation, and thermal analysis by DSC confirms the phase exclusion of both FA and RIF from PLGA as a separate amorphous phase, manifesting as surface protrusions or surface dimples, respectively (due to rapid dissolution of RIF in the forming aqueous phase). This final morphology had ultimate influence on the *in vitro* release of the drugs. Our 7 day *in vitro* release experiments indicated that the release of FA or RIF from PLGA was only achieved through a burst release, characterized by the dissolution of the surface-excluded microdomains, and was dependent on the drug(s) being excluded from the bulk of the microsphere during hardening. The release of FA and RIF was inversely related to the RIF loading in the microsphere. This was due to the observation that RIF limited the surface disposition of FA due to an increased compatibility in the PLGA matrix (i.e., a delayed phase separation). These results showed that the extent of FA or RIF burst from PLGA microspheres was controlled to a certain extent by variations in FA/RIF loadings, which govern the phase separation kinetics. These findings highlight the importance, and limitations, of polymer−drug miscibility and compatibility on the physical properties of drug-loaded polymeric microspheres.

■ ASSOCIATED CONTENT

Supporting Information

Representative XRD patterns and DSC thermograms. This material is available free of charge via the Internet at http://pubs.acs.org.

■ AUTHOR INFORMATION

Corresponding Author

*Faculty of Pharmaceutical Science, University of British Columbia, Vancouver, British Columbia V6T 1Z3, Canada. Telephone: (604) 822-2440. Fax: (604) 822-3034. E-mail: helen.burt@ubc.ca.

Notes

The authors declare no competing financial interest.

■ ACKNOWLEDGMENTS

The authors would like to thank Dr. Richard Liggins and The Center for Drug Research and Development (CDRD) for the use of their laser confocal microscope. We would also like to thank Dr. Tim Smith and Renishaw plc (Wotton-under-Edge, U.K.) for performing the Raman spectroscopy analysis on the dual-loaded microsphere formulations, and Dr. Brian Patrick and Anita Lam (UBC Chemistry) for their assistance and use of the Bruker APEX DUO diffractometer. This work would not have been possible without support from the CDRD, and a grant from the Canadian Foundation for Innovation (CFI).

■ ABBREVIATIONS

FA, fusidic acid; RIF, rifampicin; PLGA, poly(D,L-lactic acid-*co*-glycolic acid); XRPD, X-ray powder diffraction; DSC, differential scanning calorimetry; T_g, glass transition temperature; T_r, enthalpy of relaxation; ΔH_M, enthalpy of mixing; χ_{sp}, Flory−Huggins interaction parameter; VB, viscous boundary

■ REFERENCES

(1) Edlund, U.; Albertsson, A. *Degradable Polymer Microspheres for Controlled Drug Delivery—Degradable Aliphatic Polyesters*; Springer: 2002; Vol. *157*; pp 67−112.

(2) Menei, P.; Montero-Menei, C.; Venier, M. C.; Benoit, J. P. Drug delivery into the brain using poly(lactide-co-glycolide) microspheres. *Expert Opin. Drug Delivery* **2005**, *2* (2), 363−76.

(3) Patil, S. B.; Sawant, K. K. Mucoadhesive microspheres: a promising tool in drug delivery. *Curr. Drug Delivery* **2008**, *5* (4), 312−8.

(4) Reisacher, W. R.; Liotta, D. The use of poly(D,L-lactic-co-glycolic) acid microspheres in the treatment of allergic disease. *Curr. Opin. Otolaryngol. Head Neck Surg.* **2011**, *19* (3), 188−92.

(5) Sinha, V. R.; Trehan, A. Biodegradable microspheres for protein delivery. *J. Controlled Release* **2003**, *90* (3), 261−80.

(6) Tran, V. T.; Benoit, J. P.; Venier-Julienne, M. C. Why and how to prepare biodegradable, monodispersed, polymeric microparticles in the field of pharmacy? *Int. J. Pharm.* **2011**, *407* (1−2), 1−11.

(7) Letchford, K.; Sodergard, A.; Plackett, D.; Gilchrist, S.; Burt, H. Lactide and Glycolide Polymers. In *Biodegradable Polymers in Clinical Use and Clinical Development*, 1 ed.; Domb, A. J., Kumar, N., Ezra, A., Eds.; John Wiley & Sons, Inc.: 2011; pp 319−365.

(8) Yang, C.; Plackett, D.; Needham, D.; Burt, H. M. PLGA and PHBV microsphere formulations and solid-state characterization: possible implications for local delivery of fusidic acid for the treatment and prevention of orthopaedic infections. *Pharm. Res.* **2009**, *26* (7), 1644−56.

(9) Malaekeh-Nikouei, B.; Sajadi Tabassi, S. A.; Jaafari, M. R. The effect of different grades of PLGA on characteristics of microspheres encapsulated with cyclosporine A. *Curr. Drug Delivery* **2006**, *3* (4), 343−349.

(10) Passerini, N.; Craig, D. Q. M. Characterization of ciclosporin A loaded poly (D,L lactide-co-glycolide) microspheres using modulated temperature differential scanning calorimetry. *J. Pharm. Pharmacol.* **2002**, *54* (7), 913−919.

(11) Li, M.; Rouaud, O.; Poncelet, D. Microencapsulation by solvent evaporation: state of the art for process engineering approaches. *Int. J. Pharm.* **2008**, *363* (1−2), 26−39.

(12) O'Donnell, P. B.; McGinity, J. W. Preparation of microspheres by the solvent evaporation technique. *Adv. Drug Delivery Rev.* **1997**, *28* (1), 25−42.

(13) Bodmeier, R.; McGinity, J. W. The preparation and evaluation of drug-containing poly(dl-lactide) microspheres formed by the solvent evaporation method. *Pharm. Res.* **1987**, *4* (6), 465−71.

(14) Liggins, R. T.; Burt, H. M. Paclitaxel loaded poly(L-lactic acid) (PLLA) microspheres. II. The effect of processing parameters on microsphere morphology and drug release kinetics. *Int. J. Pharm.* **2004**, *281* (1−2), 103−106.

(15) Rosilio, V.; Benoit, J. P.; Deyme, M.; Thies, C.; Madelmont, G. A physicochemical study of the morphology of progesterone-loaded microspheres fabricated from poly(D,L-lactide-co-glycolide). *J. Biomed. Mater. Res.* **1991**, *25* (5), 667−82.

(16) Shenderova, A.; Burke, T. G.; Schwendeman, S. P. Stabilization of 10-hydroxycamptothecin in poly(lactide-co-glycolide) microsphere delivery vehicles. *Pharm. Res.* **1997**, *14* (10), 1406−14.

(17) Blanco-Prieto, M. J.; Durieux, C.; Dauge, V.; Fattal, E.; Couvreur, P.; Roques, B. P. Slow delivery of the selective cholecystokinin agonist pBC 264 into the rat nucleus accumbens using microspheres. *J. Neurochem.* **1996**, *67* (6), 2417−24.

(18) Janssens, S.; de Armas, H. N.; Roberts, C. J.; Van den Mooter, G. Characterization of ternary solid dispersions of itraconazole, PEG 6000, and HPMC 2910 E5. *J. Pharm. Sci.* **2008**, *97* (6), 2110−2120.

(19) Lu, Q.; Zografi, G. Phase behavior of binary and ternary amorphous mixtures containing indomethacin, citric acid, and PVP. *Pharm. Res.* **1998**, *15* (8), 1202−1206.

(20) Panyam, J.; Williams, D.; Dash, A.; Leslie-Pelecky, D.; Labhasetwar, V. Solid-state solubility influences encapsulation and release of hydrophobic drugs from PLGA/PLA nanoparticles. *J. Pharm. Sci.* **2004**, *93* (7), 1804−1814.

(21) Taepaiboon, P.; Rungsardthong, U.; Supaphol, P. Vitamin-loaded electrospun cellulose acetate nanofiber mats as transdermal and dermal therapeutic agents of vitamin A acid and vitamin E. *Eur. J. Pharm. Biopharm.* **2007**, *67* (2), 387−397.

(22) Li, W.; Anderson, K.; Deluca, P. Kinetic and thermodynamic modeling of the formation of polymeric microspheres using solvent extraction/evaporation method. *J. Controlled Release* **1995a**, *37* (3), 187−198.
(23) Li, W.; Anderson, K.; Mehta, R.; Deluca, P. Prediction of solvent removal profile and effect on properties for peptide-loaded PLGA microspheres prepared by solvent extraction/evaporation method. *J. Controlled Release* **1995b**, *37* (3), 199−214.
(24) Kunin, C. M.; Brandt, D.; Wood, H. Bacteriologic studies of rifampin, a new semisynthetic antibiotic. *J. Infect. Dis.* **1969**, *119* (2), 132−7.
(25) McCabe, W. R.; Lorian, V. Comparison of the antibacterial activity of rifampicin and other antibiotics. *Am. J. Med. Sci.* **1968**, *256* (4), 255−65.
(26) Campoccia, D.; Montanaro, L.; Arciola, C. R. The significance of infection related to orthopedic devices and issues of antibiotic resistance. *Biomaterials* **2006**, *27* (11), 2331−9.
(27) Drancourt, M.; Stein, A.; Argenson, J. N.; Roiron, R.; Groulier, P.; Raoult, D. Oral treatment of Staphylococcus spp. infected orthopaedic implants with fusidic acid or ofloxacin in combination with rifampicin. *J. Antimicrob. Chemother.* **1997**, *39* (2), 235−40.
(28) Trampuz, A.; Zimmerli, W. Antimicrobial agents in orthopaedic surgery: Prophylaxis and treatment. *Drugs* **2006**, *66* (8), 1089−105.
(29) Weber, A.; Opheim, K. E.; Smith, A. L.; Wong, K. High-pressure liquid chromatographic quantitation of rifampin and its two major metabolites in urine and serum. *Rev. Infect. Dis.* **1983**, *5* (Suppl 3), S433−9.
(30) Agrawal, S.; Ashokraj, Y.; Bharatam, P. V.; Pillai, O.; Panchagnula, R. Solid-state characterization of rifampicin samples and its biopharmaceutic relevance. *Eur. J. Pharm. Sci.: Official J. Eur. Fed. Pharm. Sci.* **2004**, *22* (2−3), 127−44.
(31) Rickard, D. L.; Duncan, P. B.; Needham, D. Hydration potential of lysozyme: protein dehydration using a single microparticle technique. *Biophys. J.* **2010**, *98* (6), 1075−1084.
(32) Duncan, P. B.; Needham, D. Microdroplet dissolution into a second-phase solvent using a micropipet technique: test of the Epstein-Plesset model for an aniline-water system. *Langmuir* **2006**, *22* (9), 4190−7.
(33) Duncan, P. B.; Needham, D. Test of the Epstein-Plesset model for gas microparticle dissolution in aqueous media: effect of surface tension and gas undersaturation in solution. *Langmuir* **2004**, *20* (7), 2567−78.
(34) Fedors, R. F. A method for estimating both the solubility parameters and molar volumes of liquids. *Polym. Eng. Sci.* **1974**, *14* (2), 147−154.
(35) Van Krevelen, D. W. *Properties of polymers*; Elsevier Science Ltd: 1997; p 875.
(36) Schenderlein, S.; Luck, M.; Muller, B. W. Partial solubility parameters of poly(D,L-lactide-co-glycolide). *Int. J. Pharm.* **2004**, *286* (1−2), 19−26.
(37) van Drooge, D. J.; Hinrichs, W. L.; Visser, M. R.; Frijlink, H. W. Characterization of the molecular distribution of drugs in glassy solid dispersions at the nanometer scale, using differential scanning calorimetry and gravimetric water vapour sorption techniques. *Int. J. Pharm.* **2006**, *310* (1−2), 220−9.
(38) Liggins, R. Paclitaxel loaded poly(L-lactic acid) microspheres: properties of microspheres made with low molecular weight polymers. *Int. J. Pharm.* **2001**, *222* (1), 19−33.
(39) Shen, E.; Kipper, M. J.; Dziadul, B.; Lim, M.-K.; Narasimhan, B. Mechanistic relationships between polymer microstructure and drug release kinetics in bioerodible polyanhydrides. *J. Controlled Release* **2002**, *82* (1), 115−125.
(40) Schott, H. Polymer Science. In *Physical pharmacy: physical chemical principles in the pharmaceutical sciences*, 4 ed.; Martin, A. N., Eds. Lea & Febiger: Philadelphia, 1969; pp 556−594.
(41) Kang, E.; Robinson, J.; Park, K.; Cheng, J. X. Paclitaxel distribution in poly(ethylene glycol)/poly(lactide-co-glycolic acid) blends and its release visualized by coherent anti-Stokes Raman scattering microscopy. *J. Controlled Release* **2007**, *122* (3), 261−8.